

Supporting information for:

Dual functional dinuclear platinum complex with selective reactivity towards c-myc G-quadruplex

Lei He,^{1a} Zhenyu Meng,^{1a} Dechen Xu¹ and Fangwei Shao^{1*}

¹Division of Chemistry and Biological Chemistry, School of Physical and Mathematical Sciences, Nanyang Technological University, 21 Nanyang Link, Singapore 637371 (Singapore)

^aThese authors contributed equally to this work

*fwshao@ntu.edu.sg

Oligonucleotides sequence

All DNA was obtained from Sangon (Shanghai, China) with HPLC purification.

ds26: 5'-CAATCGGATCGAATTCGATCCGATTG-3'.

c-myc: 5'-TGAGGGTGGGTAGGGTGGGTAA-3'.

ht21: 5'-GGGTTAGGGTTAGGGTTAGGG-3'.

rev-c-myc: 5'-ATCGCTTCTCGTCTTACCCA-3'.

rev-ht21: 5'-TCTCGTCTTCCCTAA-3'.

F-ht21-T: 5'-FAM-GGGTTAGGGTTAGGGTTAGGG-TAMRA-3'.

F-c-myc-T: 5'-FAM-TGGGGAGGGTGGGGAGGGTGGGGAAGG-TAMRA-3'.

F-bcl2-T: 5'-FAM-AGGGGCGGGCGCGGGAGGAAGGGGCGGGAGCGGGGCTG-TAMRA
-3'

F-c-kit-T: 5'-FAM-AGGGAGGGCGCTGGGAGGAGGG-TAMRA-3'.

F-duplex-T: 5'-FAM-TATAGCTATA-Spacer18-TATAGCTATA-TAMRA-3'. Spacer18 is an
18-atom hexa-ethyleneglycol spacer.

Characterization of dinuclear Pt complexes.

[{Pt(Dip)Cl}₂(μ-1,7-diaminoheptane)](NO₃)₂ (Pt1). Yield 70.4%, ESI-MS calc for [M²⁺] m/z, 628.06, found 627.53. ¹H NMR 300 MHz (CD₂Cl₂): δ 9.89 (d, *J* = 5.79 Hz, 2H, H2), δ 9.73 (d, *J* = 5.64 Hz, 2H, H9), δ 8.08 (m, 6H, H3, H5 and H6), δ 7.87(d, *J* = 5.64 Hz, 2H, H8), δ 7.62 (m, 20H, Ph), δ 5.73 (bs, 4H, NH₂), δ 3.14 (s, 4H, CH₂), δ 1.95 (s, 4H, CH₂), δ 1.48 (s, 6H, CH₂).

[{Pt(Dip)Cl}₂(μ-1,8-diaminooctane)](NO₃)₂ (Pt2). Yield 62%, ESI-MS calc for [M²⁺] m/z, 635.08, found 634.55. ¹H NMR 300 MHz (CD₂Cl₂): δ 9.84 (d, *J* = 5.67 Hz, 2H, H2), δ 9.77 (d, *J* = 5.67 Hz, 2H, H9), δ 8.08 (m, 6H, H3, H5 and H6), δ 7.90(d, *J* = 5.67 Hz, 2H, H8), δ 7.61 (m, 20H, Ph), δ 5.74 (bs, 4H, NH₂), δ 3.14 (s, 4H, CH₂), δ 1.95 (s, 4H, CH₂), δ 1.32 (s, 8H, CH₂).

[{Pt(Dip)Cl}₂(μ-1,9-diaminonoane)](NO₃)₂ (Pt3). Yield 71.3%, ESI-MS calc for [M²⁺] m/z, 642.09, found 642.65. ¹H NMR 300 MHz (CD₂Cl₂): δ 9.93 (d, *J* = 5.64 Hz, 2H, H2), δ 9.79 (d, *J* = 5.67 Hz, 2H, H9), δ 8.12 (m, 6H, H3, H5 and H6), δ 7.93(d, *J* = 5.67 Hz, 2H, H8), δ 7.65 (m, 20H, Ph), δ 5.80 (bs, 4H, NH₂), δ 3.17 (s, 4H, CH₂), δ 2.01(s, 4H, CH₂), δ 1.40 (s, 10H, CH₂).

[{Pt(Dip)Cl}₂(μ-1,10-diaminododecane)](NO₃)₂ (Pt4). Yield 56.7%, ESI-MS calc for [M²⁺] m/z, 649.10, found 649.22. ¹H NMR 300 MHz (CD₂Cl₂): δ 9.90 (d, *J* = 5.67 Hz, 2H, H2), δ 9.71 (d, *J* = 5.67 Hz, 2H, H9), δ 8.07 (m, 6H, H3, H5 and H6), δ 7.88(d, *J* = 5.67 Hz, 2H, H8), δ 7.61 (m, 20H, Ph), δ 5.79 (bs, 4H, NH₂), δ 3.12 (s, 4H, CH₂), δ 1.93(s, 4H, CH₂), δ 1.41 (s, 12H, CH₂).

Table S1. Stabilization temperature ΔT_m of different DNA structures in the presences of platinum compounds from FRET-based thermal melting.

| | ΔT_m ($^{\circ}\text{C}$) | | | | |
|------------|-------------------------------------|------|------|-------|------|
| | Pt1 | Pt2 | Pt3 | Pt4 | Pt0 |
| F-c-myc-T | 2.6 | 3.2 | 8.5 | 3.0 | 11.5 |
| F-bcl2-T | 0.6 | 0.6 | 0.8 | 0.4 | 5.0 |
| F-c-kit-T | 0.7 | 1.1 | 0.6 | 1.4 | 9.6 |
| F-ht21-T | 0.9 | 1.1 | 1.5 | 1.7 | 3.2 |
| F-duplex-T | -0.5 | -0.2 | -0.2 | -0.01 | -0.4 |

Table S2. DC_{50} (the concentration of Pt3 needed to displace 50% of thiazole orange (TO)) values for different DNA.

| DNA | DC_{50} (μM) |
|-------|------------------------------------|
| c-myc | 0.20 |
| ht21 | 1.17 |
| ds26 | 1.84 |

Table S3. Assignment for the peaks on MALDI-TOF MS spectra of peaks on HPLC of ds26 and Pt3-ds26 adducts.

| Peak | Composition | Formula | obsd | cald. |
|------|--|------------------------|---------|---------|
| D1 | ds26 | C254H321N97O154P25 | 7972.69 | 7971.24 |
| D2 | ds26 | C254H321N97O154P25 | 7971.72 | 7971.24 |
| D3 | ds26 | C254H321N97O154P25 | 7970.32 | 7971.24 |
| | ds26+Pt ₂ (Dip) ₂ (diaminonoane) | C311H371N103O154P25Pt2 | 9182.54 | 9180.46 |
| D4 | ds26+Pt ₂ (Dip) ₂ (diaminonoane) | C311H371N103O154P25Pt2 | 9181.64 | 9180.46 |

Table S4. Assignment of MALDI-TOF MS spectra for peaks on HPLC of c-myc and Pt3-GQ adducts.

| Peak | Composition | Formula | obsd | cald |
|-------|---|------------------------|---------|---------|
| c-myc | c-myc | C220H270N95O131P21 | 6991.30 | 6992.57 |
| P1 | c-myc+Pt ₂ (Dip) ₂ (diaminonoane) | C277H320N101O131P21Pt2 | 8200.74 | 8201.80 |
| P2 | c-myc+Pt ₂ (Dip) ₂ (diaminonoane) | C277H320N101O131P21Pt2 | 8201.17 | 8201.80 |

Table S5. The modified bond terms for Guanine-Pt complex

| Bond | R_0 | K_r (kJ/(nm ² *mol)) |
|-------|-------|-----------------------------------|
| N7-Pt | 2.01 | 1.5313×10^5 |

Table S6. The modified angle terms for Guanine-Pt complex

| Angle | θ_0 | K_θ (kJ/(degree*mol)) |
|------------|------------|------------------------------|
| N1'-Pt-N2' | 90 | 1.6688×10^3 |
| N1'-Pt-N3' | 180 | 1.6044×10^3 |
| N2'-Pt-N3' | 90 | 1.5382×10^3 |
| Pt-N7-C8 | 127.95 | 1.0385×10^3 |
| Pt-N7-C5 | 127.95 | 1.3339×10^3 |
| N1'-Pt-N7 | 90 | 1.3551×10^3 |
| N2'-Pt-N7 | 180 | 1.4041×10^3 |
| N3'-Pt-N7 | 90 | 1.4495×10^3 |

Table S7. The modified dihedral terms for Guanine-Pt complex

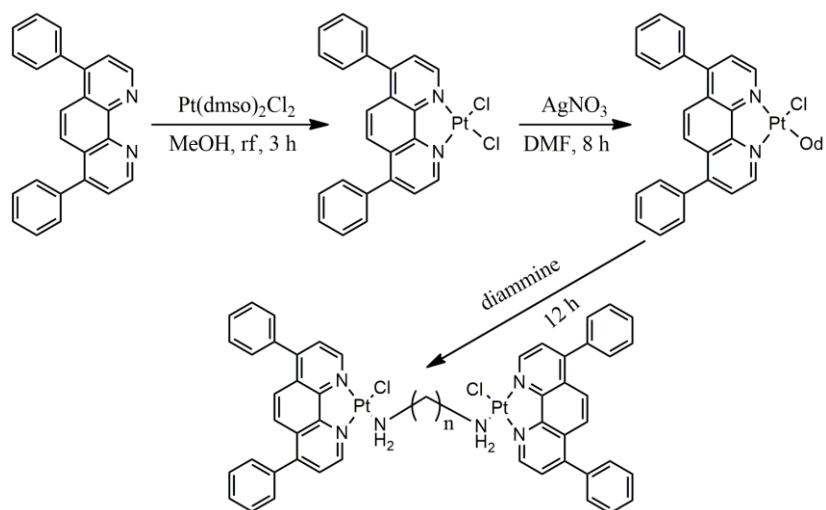
| Torsional angle | φ_0 | V_n (kJ/mol) | n |
|-----------------|-------------|----------------|-----|
| C5-C7-Pt-N1' | 90 | 2.09 | 2 |
| C8-C7-Pt-N1' | 90 | 2.09 | 2 |
| C5-C7-Pt-N2' | 90 | 2.09 | 2 |
| C8-C7-Pt-N2' | 90 | 2.09 | 2 |
| C5-C7-Pt-N3' | 90 | 2.09 | 2 |
| C8-C7-Pt-N3' | 90 | 2.09 | 2 |

Table S8 The modified improper torsional terms for Guanine-Pt complex

| Improper angle | χ_0 | K_χ (kJ/mol) |
|----------------|----------|-------------------|
| C8-C7-C5-Pt | 180 | 41.8 |

Table S9 The modified atomic charge for Guanine-Pt complex

| Atom | Atomic charge |
|--------------------|----------------------|
| N9 | -0.019 |
| C8 | 0.3057 |
| H8 | 0.069 |
| N7 | -0.3433 |
| C5 | 0.009 |
| C6 | 0.6837 |
| O6 | -0.5699 |
| N1 | -0.5053 |
| H1 | 0.352 |
| C2 | 0.7432 |
| N2 | -0.923 |
| H21 and H22 | 0.4235 |
| N3 | -0.6636 |
| C4 | 0.3847 |
| N1' | -0.11232 |
| N2' | -0.13805 |
| N3' | -0.41289 |



Scheme S1. Synthetic route of dinuclear platinum compounds, $n = 7 \sim 10$.

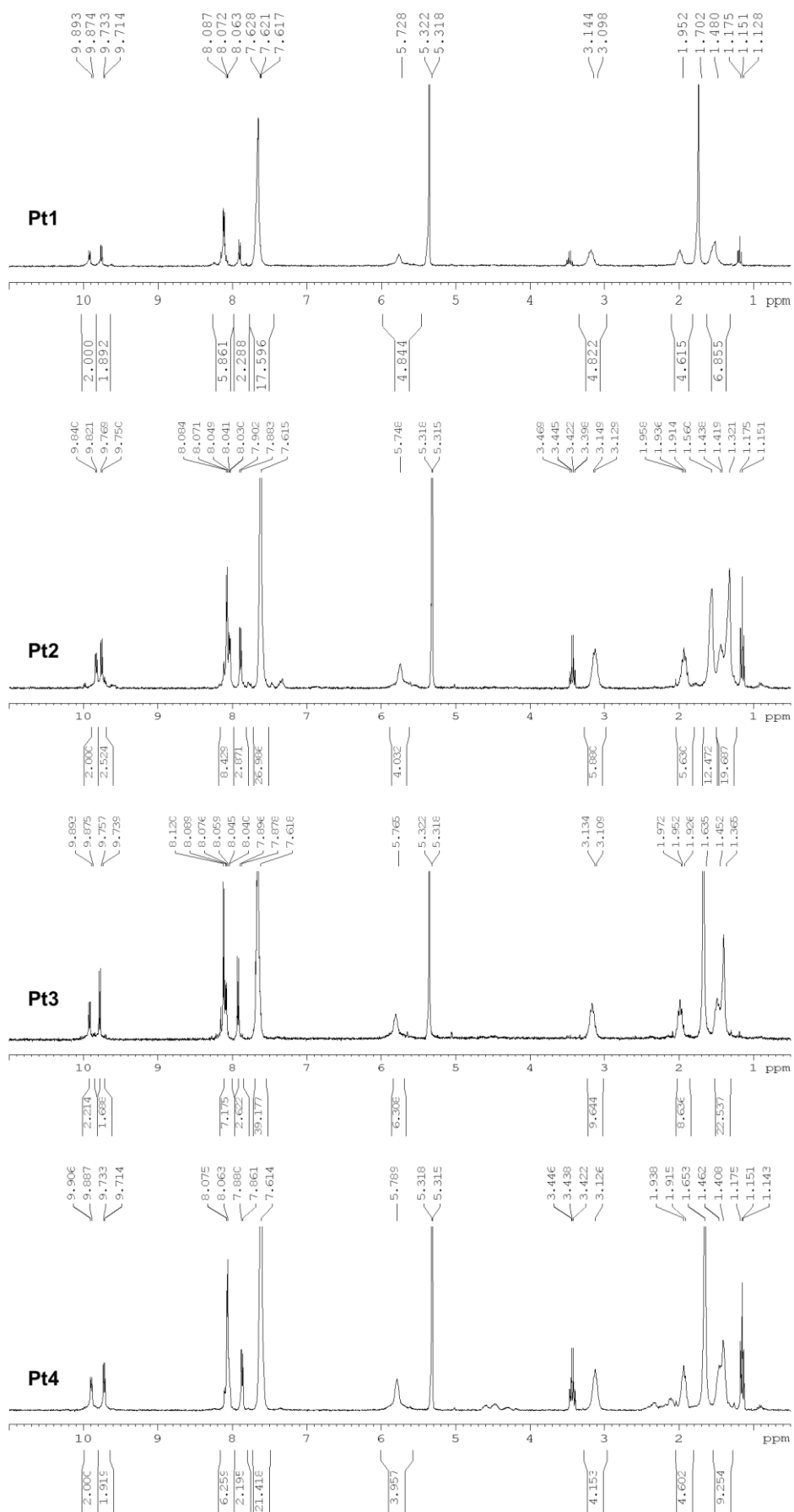


Figure S1. ^1H NMR spectrum of **Pt1-4** in CD_2Cl_2 .

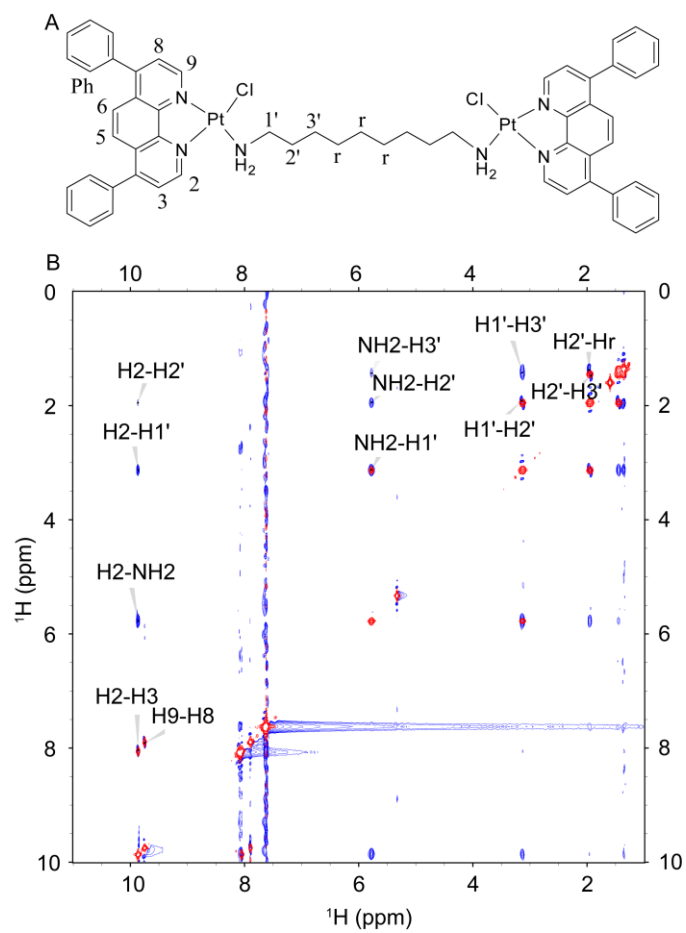


Figure S2. Overlay of ^1H - ^1H COSY (red) and ROESY (blue) spectrum of **Pt3** in CD_2Cl_2 .

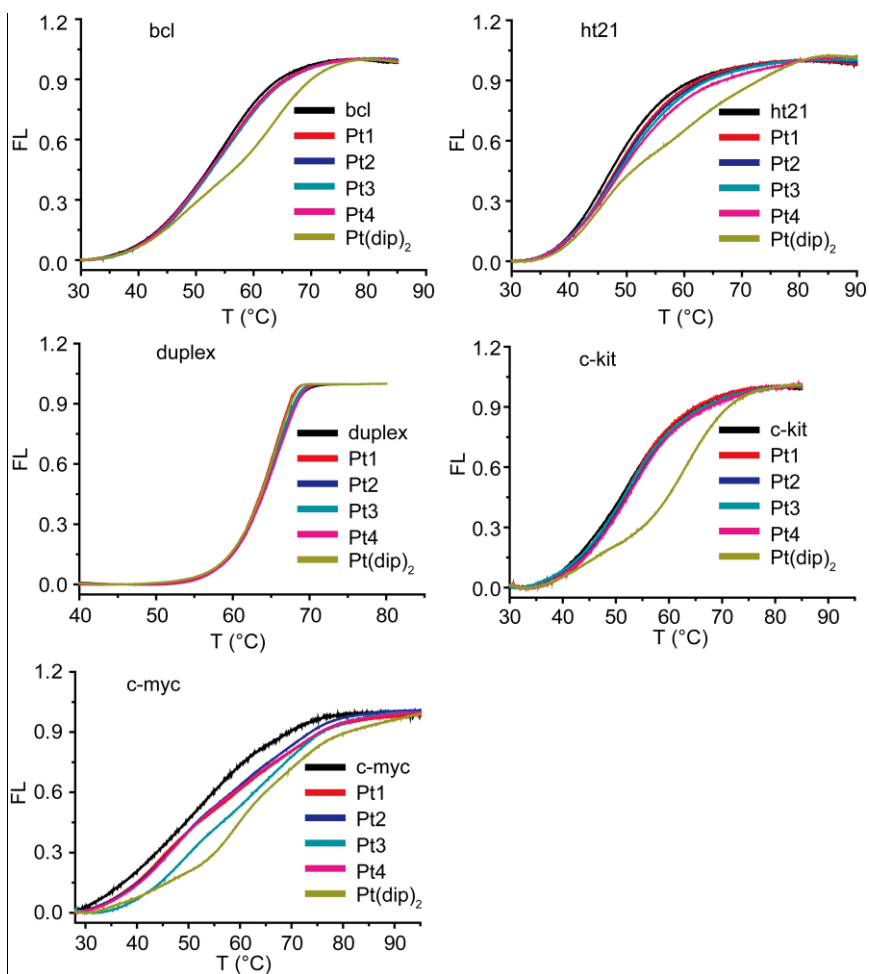


Figure S3. FRET melting profiles for 200 nM DNA without or with 200 nM different platinum compounds, in 10 mM lithium cacodylate buffer, pH 7.4, 50 mM LiCl, 5 mM KCl.

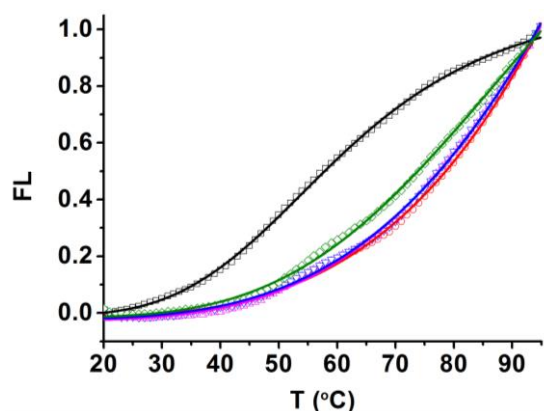


Figure S4. Competitive FRET-melting of 200 nM F-c-myc-T (black) with 1.0 μ M Pt3 and increasing amounts (0 [red], 5 [magenta] 15 [blue] and 50 [olive] equiv.) of unlabeled competitors (ds26).

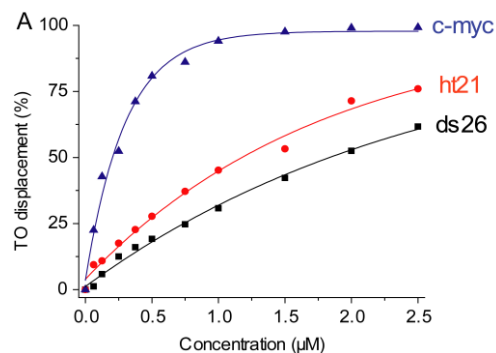


Figure S5. Plot of thiazole orange (TO) displacement vs. concentrations of **Pt3** with different DNAs.

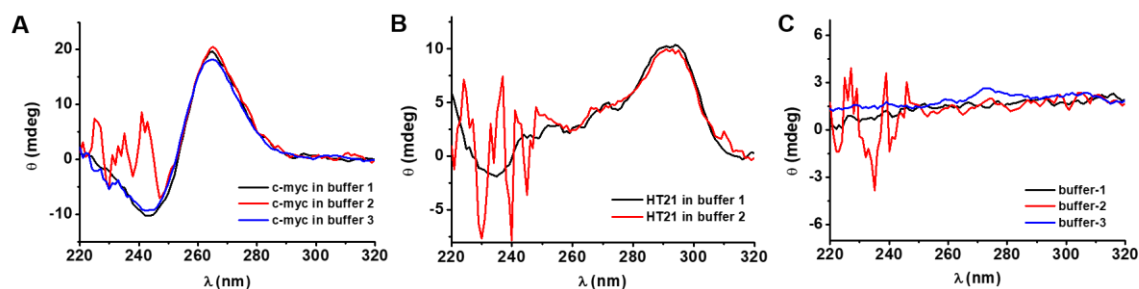


Figure S6. CD spectra of c-myc (A) and ht21 (B) in different buffers. Buffer background in CD spectra were shown in (C). **Buffer 1** is 5 mM lithium cacodylate buffer (pH 7.4) with 50 mM LiCl and 1 mM (for c-myc) or 5 mM (for ht21) KCl; **buffer 2** is 10 mM potassium phosphate buffer (pH 7.4) with 100 mM KNO₃; **buffer 3** is 1 × PCR buffer – 20 mM Tris-HCl (pH 8.4) with 50 mM KCl and 1.5 mM MgCl₂.

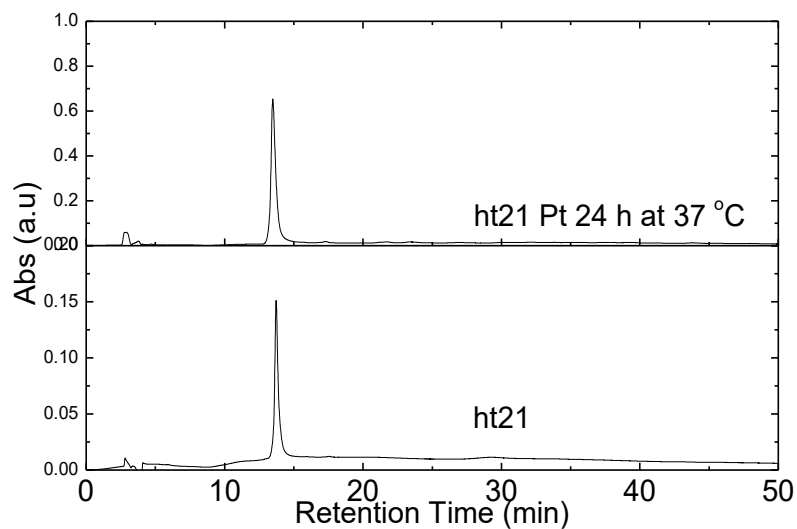


Figure S7. HPLC profiles of 10 μM ht21 G-quadruplex with or without 20 μM Pt3.

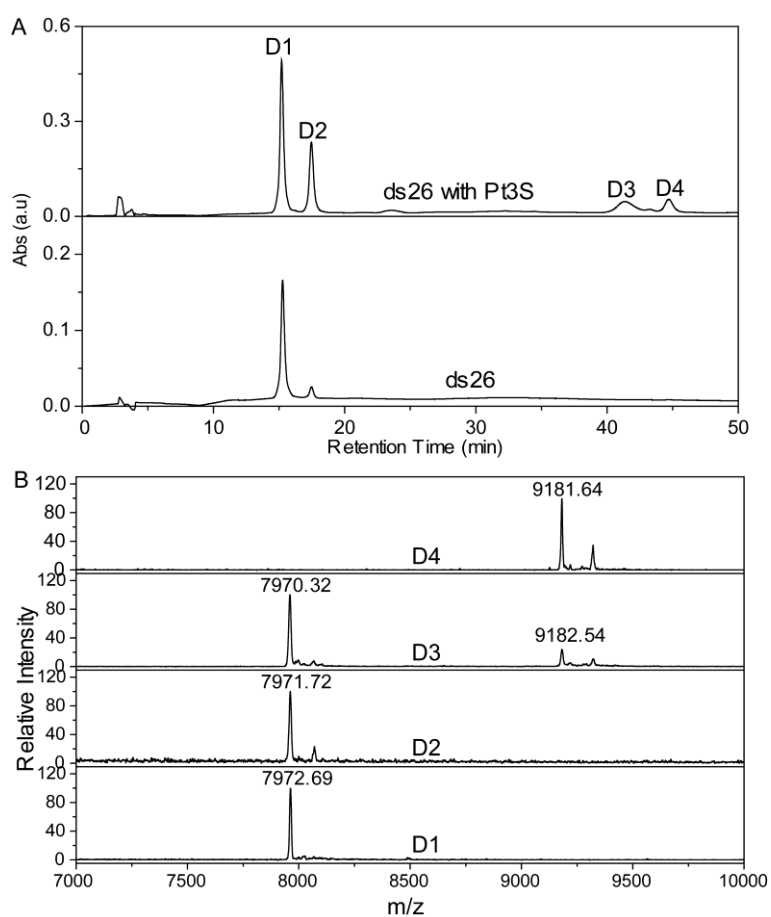


Figure S8. HPLC chromatography of ds26, and 10 μM ds26 duplex reacted with 20 μM Pt3 for 24 hours at 37 °C (A); MALDI-TOF MS spectra of peaks from HPLC (B).

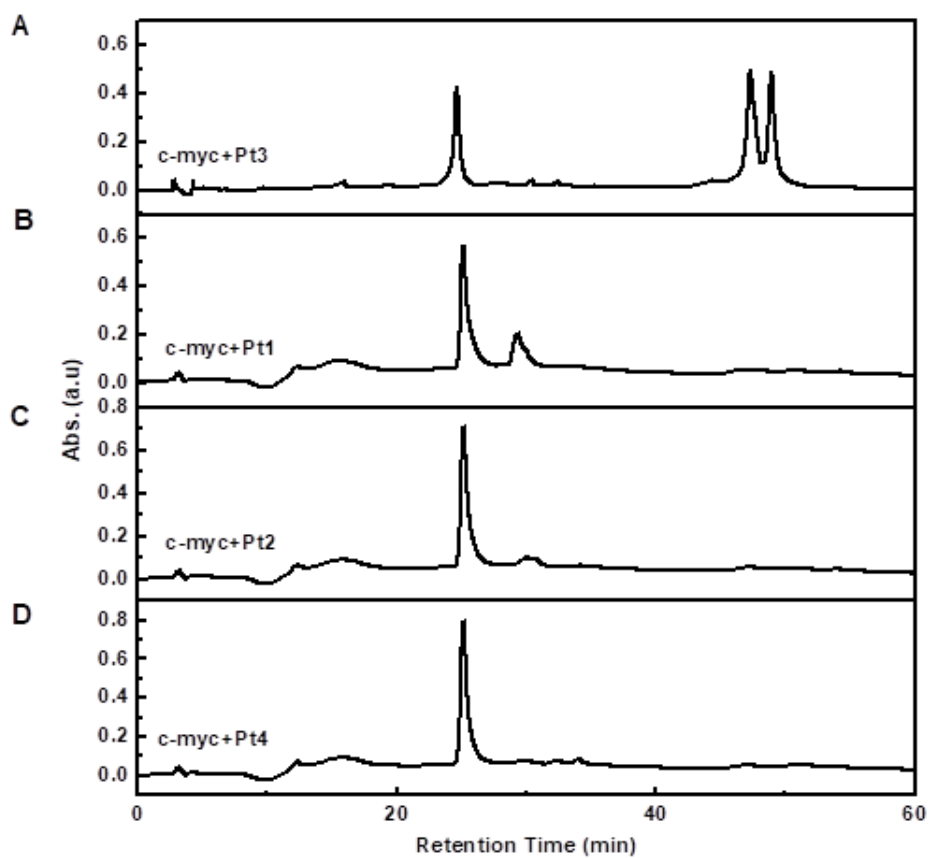


Figure S9. HPLC chromatography of c-myc, and 10 μ M c-myc reacted with 20 μ M Pt3 (A), Pt1 (B), Pt2 (C) and Pt4 (D) for 24 hours at 37 $^{\circ}$ C.

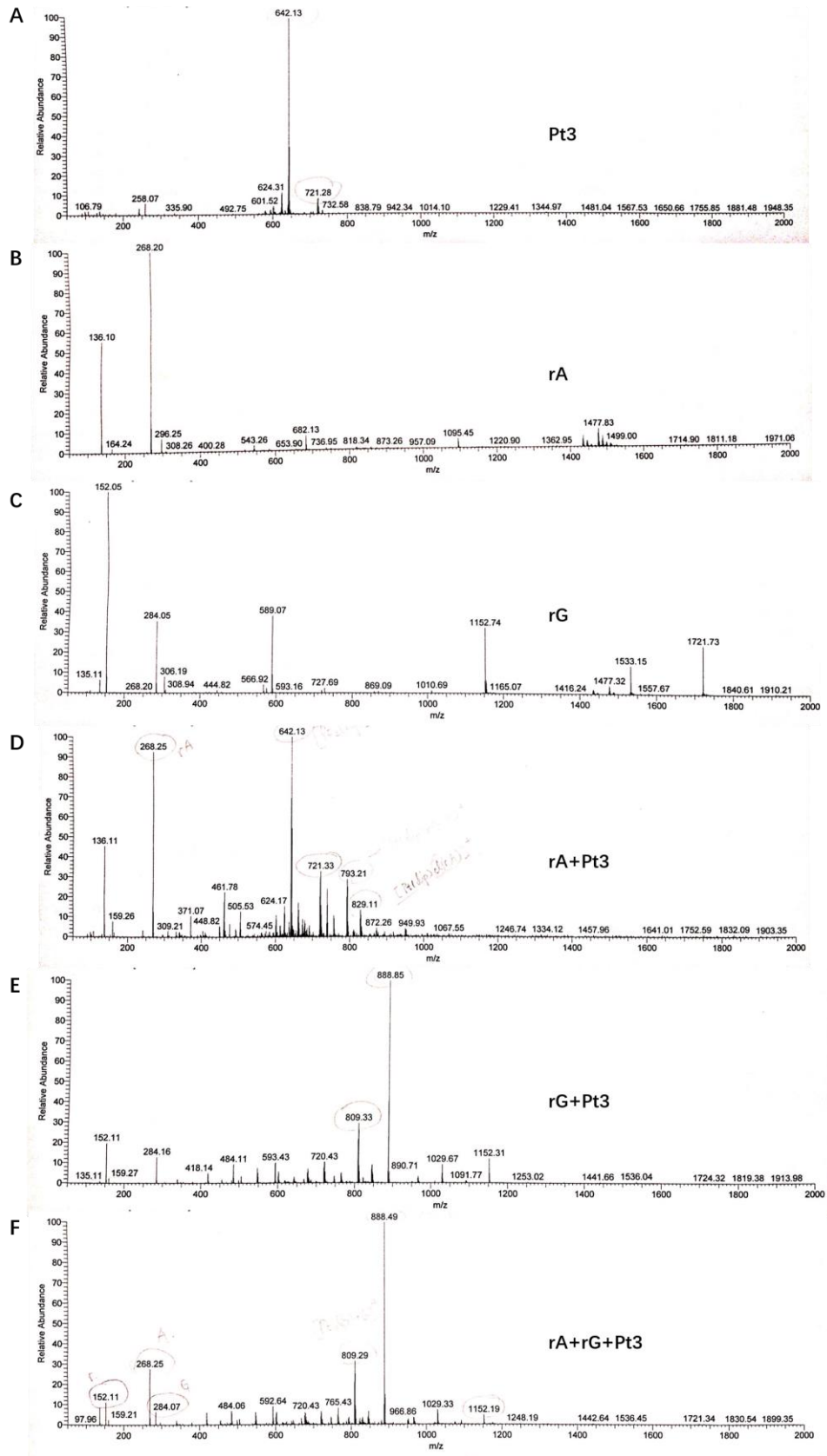


Figure S10. Mass spectrum of **Pt3** (A), adenosine (B), guanosine (C) and the adducts after 24-hour reaction. Adenosine with **Pt3** (D), guanosine with **Pt3** (E), and adenosine plus guanosine with **Pt3** (F).

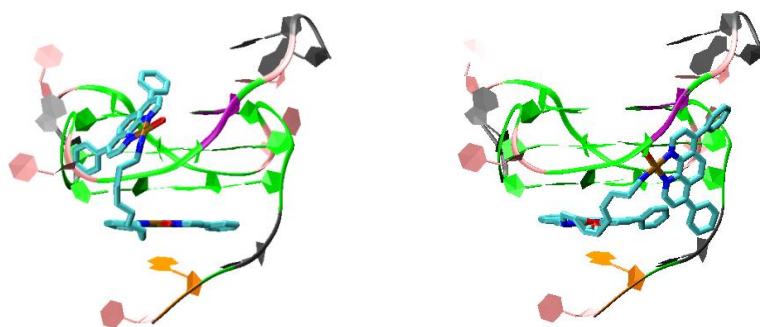


Figure S11. Molecular docking of **Pt3** to c-myc G-quadruplex. Left: Conf1; right: Conf2. The G-quadruplex was represented by new ribbon method (guanine: green; adenine: gray; thymine; pink; G2: orange; G19: purple). Complex **Pt3** was presented in Licorice method (Pt: yellow; N: navy blue; Cl: red; C: blue).

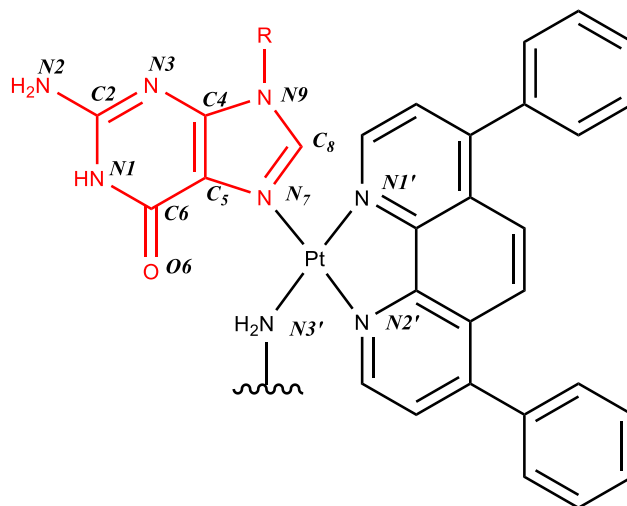
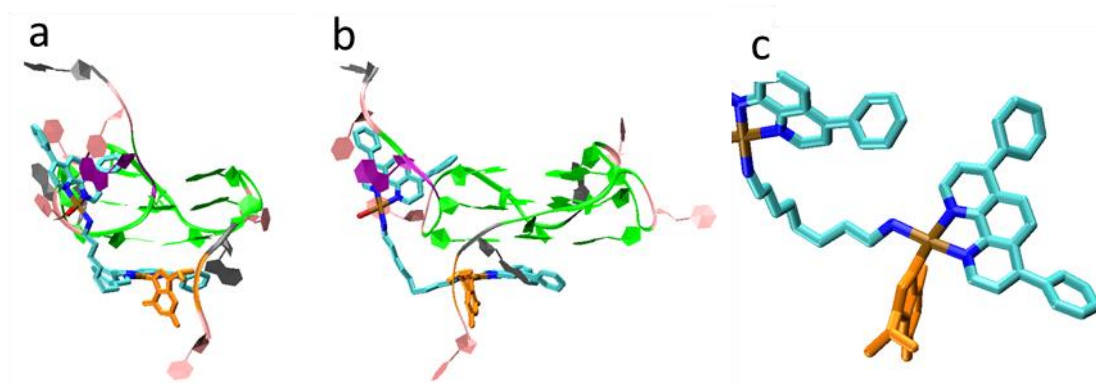


Figure S12. Structure of Pt-G complex. The atom types of coordinate atoms and guanine atoms are also labeled.



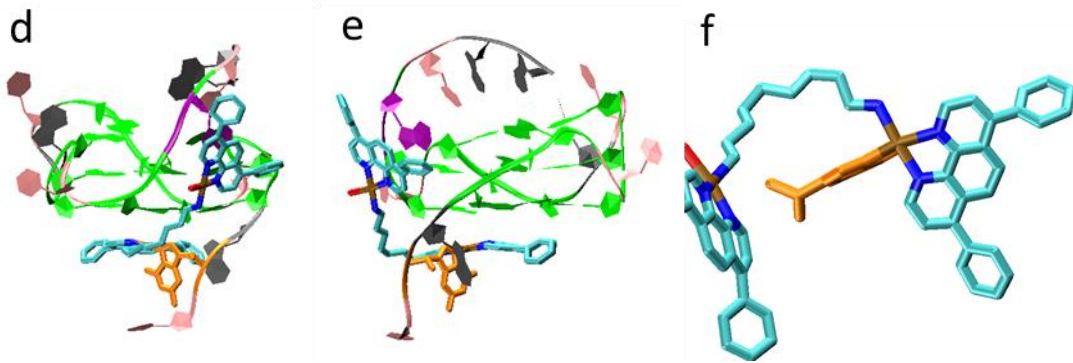


Figure S13. The structure of the two mono-crosslinked **Pt3** to c-myc GQ after 10 ns MD (a~c: Conf1; d~e: Conf2). For both conformations, the top Pt planes were close to G19 (a,d), another side view showed the top G-quartet has already decomposed under restraint (b,e). Zoom in of bottom Pt-G2 complex showed that the planar coordination geometry of Pt core has formed and G2 was nearly perpendicular to Dip ligand (c,f). The Pt complex and G2 were represented using Licorice model (Pt: brown; N: blue; C: cyan; Cl: red; guanine: orange), and the rest G-quadruplex was represented by new ribbon model (T: pink; A: gray; G: green; G2: orange; G19: purple).

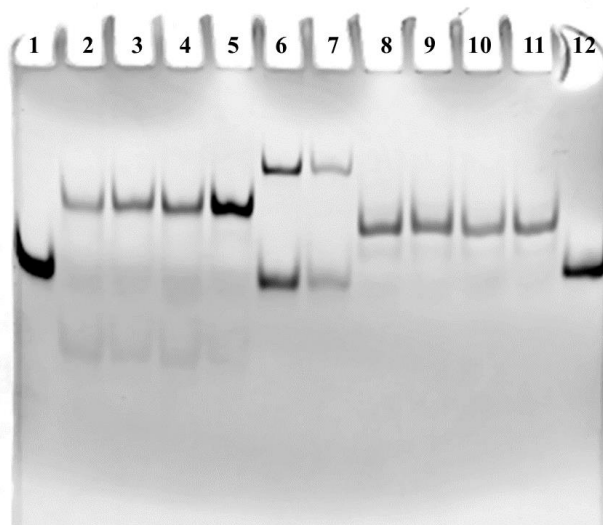


Figure S14. Inhibitory effects of **Pt3** on c-myc and ht21 templates extension in PCR-stop assay. Lane 1 and 12: control of duplex DNA – ds26; lane 6 and 7: control of both 21- and 48-mer duplex DNA; lane 5: G-rich (c-myc) sequence without **Pt3**; lane 2-4: three repeats of G-rich (c-myc) sequence with 2 equiv. amount of **Pt3**; lane 8: G-rich (ht21) sequence without **Pt3**; lane 9-11: three repeats of G-rich (ht21) sequence with 2 equiv. amount of **Pt3**.